PERGAMON

International Journal of Heat and Mass Transfer 44 (2001) 2395–2403

International Journal of HEAT and MASS TRANSFER

www.elsevier.com/locate/ijhmt

Heat transfer in microtubes with viscous dissipation

Gokturk Tunc, Yildiz Bayazitoglu *

Mechanical Engineering and Materials Science Department, Rice University, 6100 Main St., MS 321, Houston, TX 77005, USA

Received 9 June 2000; received in revised form 6 September 2000

Abstract

Convective heat transfer for steady state, laminar, hydrodynamically developed flow in microtubes with uniform temperature and uniform heat flux boundary conditions are solved by the integral transform technique. Temperature jump condition at the wall and viscous heating within the medium are included. The solution method is verified for the cases where viscous heating is neglected. For uniform temperature case, with a given Brinkman number, at specified axial lengths, the viscous effects are presented for the developing range, reaching the fully developed Nusselt number. The effect of viscous heating is investigated for both of the cases where the fluid is being heated or cooled. Prandtl number analysis has shown that, as we increase the Prandtl number the temperature jump effect diminishes which gives a rise to the Nusselt number. © 2001 Published by Elsevier Science Ltd.

1. Introduction

Experiments have shown that the fluid flow and heat transfer characteristics of microtubes deviate from well-known macroscale correlations [1,2]. As the channel size is reduced, wall effects on fluid flow and heat transfer are considerable. Molecular mean free path and channel size will have values on the same order of magnitude, allowing molecular structure to affect heat transfer. Collisions of gas molecules with the flow boundary will occur more often than those between molecules.

Typically, macrochannel boundary conditions that are applied to fluid flow and heat transfer equations, gas velocity and temperature, are equivalent to the corresponding wall values. On the contrary, these conditions are not held for rarefied gas flow in microchannels. Not only does the fluid slip along the wall with a finite tangential velocity, but also there is a jump between wall and fluid temperatures.

The Knudsen number (Kn) is used to measure rarefaction effects. Kn is defined as the ratio of molecular mean free path and the tube diameter. No-slip condition is only valid for $Kn = 0$. The continuum flow assumption holds for $Kn < 10^{-3}$ [3]. For $10^{-3} < Kn < 0.1$, the flow is called slip flow. As the flow dimension is reduced, Kn becomes larger. After a transition period, free molecular flow is experienced.

Navier–Stokes equations combined with slip flow conditions represent experimental results in microchannels for slip and moderate transition ranges [4,5]. As mentioned above, two major characteristics of slip flow are velocity slip and temperature jump at the surface. These can be determined using the kinetic theory of gases. For a cylindrical pipe, these two conditions are as:

$$\text{Velocity slip, } u_s = -\frac{2-F}{F}\lambda\left(\frac{\partial u}{\partial r}\right)_{r=R}, \tag{1}$$

where u_s is the slip velocity, λ the molecular mean free path, and F is the tangential momentum accommodation coefficient, and

$$\text{Temperature jump, } T_s - T_w = -\frac{2-F_t}{F_t}\frac{2\gamma}{\gamma+1}\frac{\lambda}{Pr}\left(\frac{\partial T}{\partial r}\right)_{r=R}, \tag{2}$$

where, T_s is the temperature of the gas at the wall, T_w the wall temperature, and F_t is the thermal accommodation coefficient. For the rest of the analysis, F and F_t will be shown by F and assumed to be 1 [6]. It is obvious from these relations that, as λ increases, velocity slip and temperature jump also increase.

* Corresponding author. Tel.: +1-713-348-6291; fax: +1-713-348-6291.

E-mail address: bayaz@rice.edu (Y. Bayazitoglu).

0017-9310/01/$ - see front matter © 2001 Published by Elsevier Science Ltd.
PII: S0017-9310(00)00298-2

Nomenclature

Br	Brinkman number, $Br = EcPr$
c_p	specific heat, J/kg K
D	tube diameter, m
Ec	Eckert number, $Ec = u_m^2/c_p\Delta T$
F	tangential momentum accommodation coefficient
F_t	thermal accommodation coefficient
Gz	Graetz number
h	heat transfer coefficient, W/m^2 K
k	thermal conductivity, W/m K
Kn	Knudsen number
L	tube length, m
N	normalization integral
Nu	Nusselt number, hD/k
Pr	Prandtl number, v/α
R	tube radius, m
r	radial coordinate
Re	Reynolds number, $\rho u_m D/\mu$
T	fluid temperature, K
u	fluid velocity, m/s
x	axial coordinate

Greek symbols

α	thermal diffusivity, m^2/s
γ	specific heat ratio
ϕ	a variable that is used to define the temperature in the developing range
λ	eigenvalue, molecular mean free path
μ	dynamic viscosity, kg/ms
v	kinematic viscosity, m^2/s
ψ	eigenfunction
ρ	density, kg/m^3
θ	non-dimensional temperature
η	non-dimensional radial coordinate
ζ	non-dimensional axial coordinate

Subscripts

b	bulk properties
m	average values
s	fluid properties at the wall
w	wall values
0	inlet properties

Superscript

$*$	non-dimensional variables

Sparrow and Lin [7] states that the Nusselt number decreases with increasing Knudsen number for both constant temperature and constant heat flux boundary conditions. The reduction is strongly influenced by the increased temperature jump. He also states that the entrance length varies with Kn; as Kn increases, entrance length becomes larger.

Barron et al. [6] and Ameel et al. [8] solve the problem for $0 < Kn < 0.12$ with uniform temperature and uniform heat flux boundary conditions, respectively. In the former case, he finds that the Nusselt number increases as the wall boundary conditions move further from the traditional no-slip condition, whereas the latter shows an opposite effect.

Kavehpour et al. [9] solves the compressible forms of the momentum and energy equations with slip velocity and temperature jump boundary conditions in a parallel plate channel. The effect of compressibility is important for higher Re and that the effect of rarefaction is significant for lower Re. The Nusselt number is substantially lower for slip flows compared to that for continuum flows.

2. Analysis

2.1. Uniform temperature

We start the analysis with the two-dimensional energy equation. The fluid properties are assumed to be constant. Since the fluid next to wall has a temperature finitely different from the wall temperature, slip temperature should be used for the first boundary condition. The second and third boundary conditions are centerline symmetry and uniform temperature at the channel entrance.

$$u\frac{\partial T}{\partial x} = \frac{\alpha}{r}\frac{\partial}{\partial r}\left(r\frac{\partial T}{\partial r}\right) + \frac{v}{c_p}\left(\frac{\mathrm{d}u}{\mathrm{d}r}\right)^2, \tag{3a}$$

$$T = T_s \quad \text{at } r = R, \tag{3b}$$

$$\frac{\partial T}{\partial r} = 0 \quad \text{at } r = 0, \tag{3c}$$

$$T = T_0 \quad \text{at } x = 0. \tag{3d}$$

The fully developed velocity profile for slip flow is derived from the momentum equation using the slip velocity.

$$u = \frac{2u_m(1 - (r/R)^2 + 4Kn)}{(1 + 8Kn)}, \tag{4}$$

where u_m is the mean velocity and $Kn = \lambda/D$.Then temperature, spatial variables, and velocity are non-dimensionalized by the temperature of the fluid at the wall, T_s, tube radius and length, and mean velocity.

$$\theta = \frac{T - T_s}{T_0 - T_s}, \quad \eta = \frac{r}{R}, \quad \zeta = \frac{x}{L}, \quad u^* = \frac{u}{u_m}. \tag{5}$$

The energy equation is obtained in the following form after introducing non-dimensional parameters

$$\frac{Gz(1-\eta^2+4Kn)}{2(1+8Kn)}\frac{\partial\theta}{\partial\zeta}=\frac{1}{\eta}\frac{\partial}{\partial\eta}\left(\eta\frac{\partial\theta}{\partial\eta}\right)+\frac{16Br}{(1+8Kn)^2}\eta^2, \tag{6a}$$

where the Graetz number and the Brinkman number are defined as

$$Gz=\frac{RePrD}{L} \quad \text{and} \quad Br=\frac{\mu u_m^2}{k\Delta T},$$

where ΔT is the difference between the temperature of the fluid at the wall and the tube entrance, $\Delta T = T_0 - T_s$. The boundary and initial conditions are also non-dimensionalized by the same parameters as follows:

$$\theta=0 \quad \text{at} \quad \eta=1, \tag{6b}$$

$$\frac{\partial\theta}{\partial\eta}=0 \quad \text{at } \eta=0, \tag{6c}$$

$$\theta=1 \quad \text{at } \zeta=0. \tag{6d}$$

The integral transform technique, a straightforward analytical solution technique, is applied. The fundamentals of this technique are obtained from the separation of variables method [10,11]: First, an appropriate integral transform pair is developed. Then, by transformation, the partial derivative with respect to ζ is removed from the governing equation, reducing the governing equation to an ordinary differential equation. Finally, the resulting ODE is solved subject to the transformed initial condition. The temperature distribution is then obtained by applying the inversion formula to the transform of temperature.

The following eigenvalue problem is chosen to develop the solution method.

$$\frac{1}{\eta}\frac{\partial}{\partial\eta}\left(\eta\frac{\mathrm{d}\psi}{\mathrm{d}\eta}\right)+(1-\eta^2+4Kn)\lambda_m^2\psi=0, \tag{7a}$$

$$\frac{\mathrm{d}\psi}{\mathrm{d}\eta}=0 \quad \text{at } \eta=0, \tag{7b}$$

$$\psi=0 \quad \text{at } \eta=1. \tag{7c}$$

In the above problem definition, $\psi(\lambda_m,\eta)$'s and λ_m's are the eigenfunctions and eigenvalues. Now, we define the orthogonality condition of the eigenfunctions

$$\int_0^1 \eta(1-\eta^2+4Kn)\psi(\lambda_m,\eta)\psi(\lambda_n,\eta)\,\mathrm{d}\eta = \begin{cases} 0 & \text{for } m\neq n, \\ N(\lambda_m) & \text{for } m=n, \end{cases} \tag{8}$$

where the normalization integral, $N(\lambda_m)$ is calculated from the following formula:

$$N(\lambda_m)=\int_0^1 \eta(1-\eta^2+4Kn)[\psi(\lambda_m,\eta)]^2\,\mathrm{d}\eta. \tag{9}$$

Then the integral transform pair can be written as:

$$\text{Transform: } \overline{\theta}(\lambda_m,\zeta)=\int_0^1 \eta(1-\eta^2+4Kn)\times\psi(\lambda_m,\eta)\theta(\eta,\zeta)\,\mathrm{d}\eta, \tag{10}$$

$$\text{Inversion: } \theta(\eta,\zeta)=\sum_{m=1}^{\infty}\frac{1}{N(\lambda_m)}\psi(\lambda_m,\eta)\overline{\theta}(\lambda_m,\zeta). \tag{11}$$

We now take the transformation of equation (6a). Both sides of the equation are multiplied by $\eta\psi(\lambda_m,\eta)$ and integrated over the domain, $\eta\in[0,1]$. We use Green's theorem to evaluate the transformation of the second-order partial derivative in Eq. (6a). Then, the eigenvalue problem and the boundary conditions of both the governing equation and the eigenvalue problem are utilized. Finally, we obtain the corresponding ODE in the following form:

$$\frac{\mathrm{d}\overline{\theta}_m}{\mathrm{d}\zeta}+\frac{2(1+8Kn)}{Gz}\lambda_m^2\overline{\theta}_m=\frac{32Br}{Gz(1+8Kn)}\int_0^1\eta^3\psi(\lambda_m,\eta)\,\mathrm{d}\eta. \tag{12}$$

We note here that the parameter for which we are trying to solve is the transformed temperature.

The solution to Eq. (12) is easily written as

$$\overline{\theta}_m=\frac{K_m}{P_m}+c\mathrm{e}^{-P_m\zeta}, \tag{13}$$

where

$$K_m=\frac{32Br}{Gz(1+8Kn)}\int_0^1\eta^3\psi(\lambda_m,\eta)\,\mathrm{d}\eta$$

and

$$P_m=\frac{2(1+8Kn)}{Gz}\lambda_m^2$$

c is determined from the initial condition, Eq. (6d), as

$$c=\overline{1}_m-\frac{K_m}{P_m}, \tag{14}$$

where $\overline{1}_m$ is the integral transformation of the initial condition and is calculated from

$$\overline{1}_m=\int_0^1\eta(1-\eta^2+4Kn)\psi(\lambda_m,\eta)\,\mathrm{d}\eta. \tag{15}$$

Then the transformed temperature distribution takes the following form:

$$\overline{\theta}_m = \frac{16Br\int_0^1 \eta^3\psi(\lambda_m,\eta)\,\mathrm{d}\eta}{(1+8Kn)^2\lambda_m^2} + \left(\int_0^1 \eta(1-\eta^2+4Kn)\psi(\lambda_m,\eta)\,\mathrm{d}\eta - \frac{16Br\int_0^1 \eta^3\psi(\lambda_m,\eta)\,\mathrm{d}\eta}{(1+8Kn)^2\lambda_m^2}\right)\mathrm{e}^{-P_m\zeta}. \tag{16}$$

By introducing Eq. (16) into the inversion formula, the non-dimensional temperature field becomes

$$\theta(\eta,\zeta) = \sum_{m=1}^{\infty} \frac{\psi(\lambda_m,\eta)}{\int_0^1 \eta(1-\eta^2+4Kn)[\psi(\lambda_m,\eta)]^2\,\mathrm{d}\eta} \times \left(\frac{16Br\int_0^1 \eta^3\psi(\lambda_m,\eta)\,\mathrm{d}\eta}{(1+8Kn)^2\lambda_m^2} + \left(\int_0^1 \eta(1-\eta^2+4Kn)\psi(\lambda_m,\eta)\,\mathrm{d}\eta - \frac{16Br\int_0^1 \eta^3\psi(\lambda_m,\eta)\,\mathrm{d}\eta}{(1+8Kn)^2\lambda_m^2}\right)\mathrm{e}^{-P_m\zeta}\right). \tag{17}$$

The only unknowns in Eq. (17) are $\psi(\lambda_m,\eta)$ and λ_m, which are obtained by solving the eigenvalue problem. Once they are evaluated, the normalization integral and the transformation of the initial condition are calculated and substituted into Eq. (17).

We now derive an expression for the local Nusselt number considering the temperature jump. First, the local heat transfer rate is written in two different ways and then equated to solve for the heat convection coefficient.

Heat transfer from the fluid to the wall by convection is written as

$$q_x = h_x(T_\mathrm{b} - T_\mathrm{w}). \tag{18}$$

Heat flux at the wall can also be written using Fourier's law

$$q_x = -k\left.\frac{\partial T}{\partial r}\right|_{r=R}. \tag{19}$$

Equating these two yields

$$h_x = -\frac{k}{(T_\mathrm{b}-T_\mathrm{w})}\left.\frac{\partial T}{\partial r}\right|_{r=R} \tag{20}$$

and in the following non-dimensional form

$$h_x = -\frac{(k/R)}{\{(T_\mathrm{b}-T_\mathrm{s})/(T_0-T_\mathrm{s})\}-\{(T_\mathrm{w}-T_\mathrm{s})/(T_0-T_\mathrm{s})\}}\left.\frac{\partial\theta}{\partial\eta}\right|_{\eta=1}. \tag{21}$$

The first term in the denominator is θ_b by definition. The second term, however, has to be determined from the temperature jump boundary condition, which is given by Eq. (2). We write the jump condition in the following dimensionless form:

$$\frac{T_\mathrm{s}-T_\mathrm{w}}{T_0-T_\mathrm{s}} = -\frac{4\gamma}{\gamma+1}\frac{Kn}{Pr}\left.\frac{\partial\theta}{\partial\eta}\right|_{\eta=1}. \tag{22}$$

Substituting Eq. (22) into Eq. (21) results in the final form of the heat convection coefficient

$$h_x = -\frac{k}{R\left(\theta_\mathrm{b} - \frac{4\gamma}{\gamma+1}\frac{Kn}{Pr}\left.\frac{\partial\theta}{\partial\eta}\right|_{\eta=1}\right)}\left.\frac{\partial\theta}{\partial\eta}\right|_{\eta=1}, \tag{23}$$

where the bulk temperature is defined as

$$\theta_\mathrm{b} = 2\int_0^1 \left(\frac{u}{u_m}\right)\theta(\eta,\zeta)\eta\,\mathrm{d}\eta.$$

The Nusselt number is now easily determined as follows:

$$Nu_x = \frac{h_x D}{k} = -\frac{2\left.\frac{\partial\theta}{\partial\eta}\right|_{\eta=1}}{\left(\theta_\mathrm{b} - \frac{4\gamma}{\gamma+1}\frac{Kn}{Pr}\left.\frac{\partial\theta}{\partial\eta}\right|_{\eta=1}\right)}. \tag{24}$$

2.2. Uniform heat flux

The energy equation for the uniform temperature case is used with small modifications. The definition of θ and Br are as follows:

$$\theta = \frac{T-T_0}{q''R/k} \quad \text{and} \quad Br = \frac{\mu u_m^2}{q''D}.$$

Substitution of these into energy equation yields

$$\frac{Gz(1-\eta^2+4Kn)}{2(1+8Kn)}\frac{\partial\theta}{\partial\zeta} = \frac{1}{\eta}\frac{\partial}{\partial\eta}\left(\eta\frac{\partial\theta}{\partial\eta}\right) + \frac{32Br}{(1+8Kn)^2}\eta^2. \tag{25}$$

Centerline symmetry and uniform initial temperature conditions are the same, however wall boundary condition is given by

$$\left.\frac{\partial\theta}{\partial\eta}\right|_{\eta=1} = 1.$$

We define a new variable, ϕ, as the difference between the temperature profile and the fully developed temperature profile.

$$\phi(\eta,\zeta) = \theta(\eta,\zeta) - \theta_\infty(\eta,\zeta), \tag{26}$$

where the fully developed temperature profile is derived as

$$\phi_\infty = 4\zeta + \left(1+\frac{C_{Br}}{4}\right)\frac{(\eta^2-(\eta^4/4)+4Kn\eta^2)}{(1+8Kn)} - \frac{(4+C_{Br})(7+112Kn+384Kn^2)}{C_{Br}(1+8Kn)^2} - \frac{96\eta^4}{16} + \frac{C_{Br}(1+16Kn)}{96(1+8Kn)} \tag{27}$$

with

$$\left.\frac{\partial\theta_\infty}{\partial_\eta}\right|_{\eta=0}=0 \quad \text{and} \quad \left.\frac{\partial\theta_\infty}{\partial_\eta}\right|_{\eta=1}=1,$$

where

$$C_{Br}=\frac{32Br}{(1+8Kn)^2}.$$

The following equation system, which is obtained after the substitution of $\theta=\phi+\theta_\infty$ into the energy equation, is satisfied by ϕ

$$\frac{Gz(1-\eta^2+4Kn)}{2(1+8Kn)}\frac{\partial\phi}{\partial\zeta}=\frac{1}{\eta}\frac{\partial}{\partial\eta}\left(\eta\frac{\partial\phi}{\partial\eta}\right)+\frac{32Br}{(1+8Kn)^2}\eta^2, \tag{28}$$

$$\frac{\partial\phi}{\partial\eta}=0 \quad \text{at } \eta=0,$$

$$\frac{\partial\phi}{\partial\eta}=0 \quad \text{at } \eta=1,$$

$$\phi=\phi_0=-\theta_\infty \quad \text{at } \zeta=0.$$

We apply the same procedure to solve for ϕ. The boundary conditions of the eigenvalue problem change. The following eigenvalue problem is solved in this case

$$\frac{1}{\eta}\frac{\partial}{\partial\eta}\left(\eta\frac{\mathrm{d}\psi}{\mathrm{d}\eta}\right)+(1-\eta^2+4Kn)\lambda_m^2\psi=0, \tag{29}$$

$$\frac{\mathrm{d}\psi}{\mathrm{d}\eta}=0 \quad \text{at } \eta=0,$$

$$\frac{\mathrm{d}\psi}{\mathrm{d}\eta}=0 \quad \text{at } \eta=1.$$

The solution for the transform of ϕ, is obtained similar to Eq. (13)

$$\overline{\phi}_m=\frac{K_m}{P_m}-\left(\overline{\phi}_0+\frac{K_m}{P_m}\right)\mathrm{e}^{-P_m\zeta}, \tag{30}$$

where

$$K_m=\frac{64Br}{Gz(1+8Kn)}\int_0^1\eta^3\psi(\lambda_m,\eta)\,\mathrm{d}\eta$$

and $\quad P_m=\dfrac{2(1+8Kn)}{Gz}\lambda_m^2$

and

$$\overline{\phi}_0=\int_0^1\eta(1-\eta^2+4Kn)\left(\left(1+\frac{C_{Br}}{4}\right)\times\frac{(\eta^2-(\eta^4/4)+4Kn\eta^2)}{(1+8Kn)}-\frac{(4+C_{Br})7+112Kn+384Kn^2}{96(1+8Kn)^2}-\frac{C_{Br}\eta^4}{16}+\frac{C_{Br}(1+16Kn)}{96(1+8Kn)}\right)\psi(\lambda_m,\eta)\,\mathrm{d}\eta. \tag{31}$$

Then, the inversion formula, Eq. (11) is applied to obtain ϕ. Finally, the temperature profile is obtained by adding ϕ and θ_∞.

After we obtain the temperature profile, the Nusselt number is calculated by using the following expression similar to the previous case

$$Nu_x=\frac{2}{\theta_\mathrm{s}+\{(4\gamma/(\gamma+1))(Kn/Pr)\}-\theta_\mathrm{b}}. \tag{32}$$

3. Results and discussion

In this section, we are going to present the effects of the Knudsen number and the Brinkman number on heat transfer. The Prandtl number is also an important parameter for the Nusselt number values, which are directly proportional to the temperature difference between the fluid and the wall. Therefore, we will also discuss the variation of Nu with Pr.

We computed the fully developed Nusselt numbers for $0<Kn<0.12$, $Pr=0.7$, and $Br=0$. The results are shown in Tables 1 and 3 for two different boundary conditions. The fully developed Nusselt number decreases as Kn increases. For the no-slip

Table 1
The fully developed Nusselt number values, $Br=0$, constant T at the wall

$Br=0$	$Pr=0.6$	$Pr=0.7$	$Pr=0.8$	$Pr=0.9$	$Pr=1.0$
$Kn=0.0$	3.6751	3.6751	3.6751	3.6751	3.6751
$Kn=0.02$	3.3675	3.4317	3.4814	3.5212	3.5536
$Kn=0.04$	3.0745	3.1833	3.2700	3.3408	3.3997
$Kn=0.06$	2.8101	2.9482	3.0610	3.1549	3.2342
$Kn=0.08$	2.5767	2.7332	2.8636	2.9740	3.0687
$Kn=0.10$	2.3723	2.5397	2.6816	2.8034	2.9091
$Kn=0.12$	2.1937	2.3667	2.5156	2.6449	2.7584

condition $Nu_\infty = 3.6751$, while it drops down to 2.3667 for $Kn = 0.12$, a decrease of 35.6%. This is due to the fact that the temperature jump reduces heat transfer. As Kn increases, the temperature jump also increases. Therefore, the denominator of Eq. (24) takes larger values. Similar results were found in [7]. They report approximately a 32% decrease. However, in [6], the Graetz problem is extended to slip flow, where they find an increase in the Nusselt number for the same conditions without considering the temperature jump. Table 3 also indicates a decrease in Nu with increasing Kn. In this case Nu drops 38.6%, from 4.363 to 2.681. Ameel et al. [8] and Sparrow and Lin [7] report similar results.

In Fig. 1, we show the effect of temperature jump on the Nusselt number clearly. The solid and dashed lines represent the results from the present study for constant heat flux and constant temperature boundary conditions, respectively, whereas; squares and diamonds show the data from Barron et al. [6] and Ameel et al. [8]. When the temperature jump condition is not considered, in other words, only the velocity slip condition is taken into account, the Nusselt number increases with increasing Kn, which implies that the velocity slip and temperature jump have opposite effects on the Nusselt number.

In Fig. 2, we show the Nusselt number values in the thermally developing range. For both of the cases, as Kn increases, the Nusselt number decreases due to the increasing temperature jump. We note here that, the decrease is greater when we consider viscous dissipation. While the fully developed Nusselt number for no-slip condition is 6.4231 for $Br = 0.01$, it is 3.0729 for $Kn = 0.12$ (52.2% decrease as opposed to 35.6% decrease for no-viscous heating case).

Next we looked at the variation of the fully developed Nusselt number with the Prandtl number. The results can be seen in Fig. 3. The lines represent the same

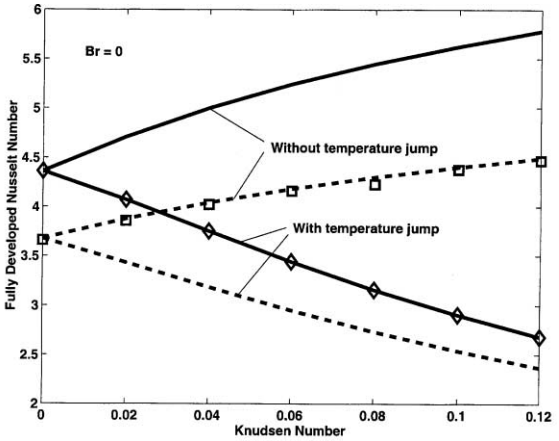

Fig. 1. The effect of temperature jump on heat transfer.

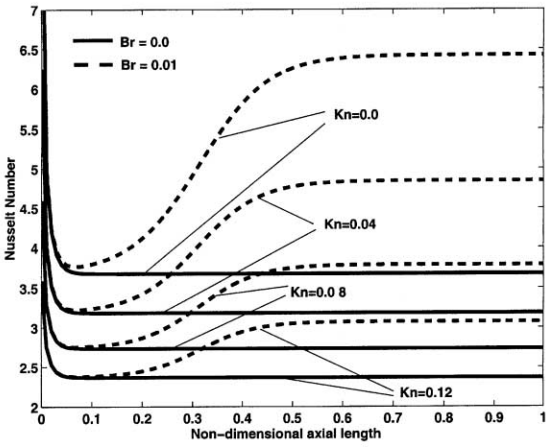

Fig. 2. Variation of the Nusselt number with the Knudsen number at the entrance region for uniform temperature at the wall.

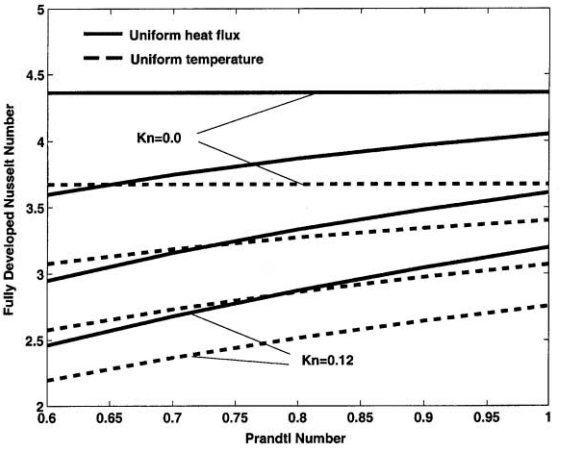

Fig. 3. The effect of the Prandtl number on the Nusselt number under the slip flow conditions.

corresponding values of Kn as those in Fig. 2. Since Pr tends to decrease the temperature jump by definition (Eq. (2)), it increases the Nusselt number according to the statement given above. With the uniform temperature boundary condition, while there is a 40% decrease in Nu for $Pr = 0.6$, the decrease is 24.9% when $Pr = 1$. With the uniform heat flux boundary condition Nu decreases 43.6% and 26.8% for $Pr = 0.6$ and $Pr = 1$, respectively.

In the following figures, the effect of viscous heating combined with the slip flow will be presented in more detail. In Fig. 4, the results for $Kn = 0.04$ and $Pr = 0.7$ are seen where the bottom curve represents no-viscous dissipation condition. The results are given for $0 \leqslant Br \leqslant 0.015$. Including the Brinkman number causes

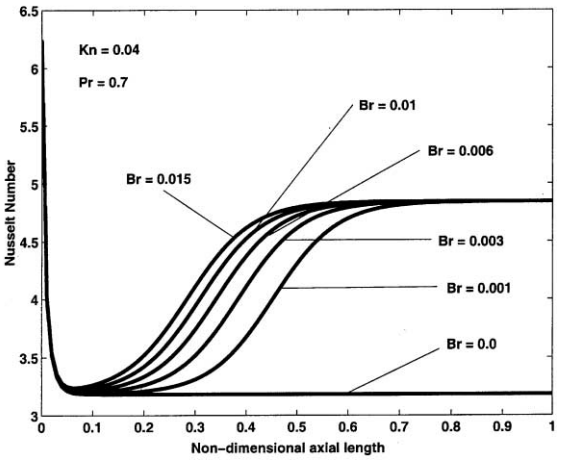

Fig. 4. The effect of viscous heating on heat transfer at the channel entrance for uniform temperature at the wall.

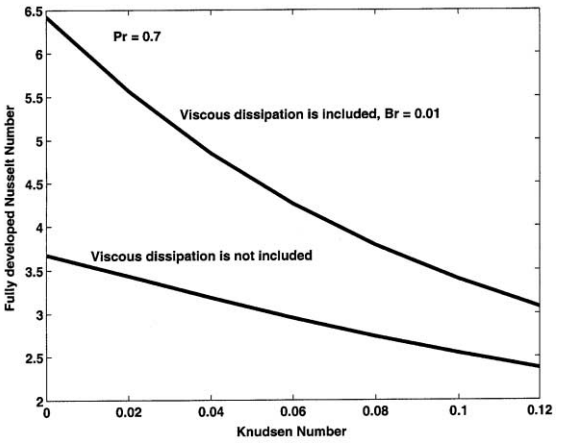

Fig. 6. Variation of the fully developed Nusselt number with Knudsen number with/without considering viscous heating for uniform temperature at the wall.

an increase in *Nu*. In this case, *Nu* goes from 3.1833 to 4.8446. The system first reaches the fully developed condition as if there is no viscous heating. Then, at some point, *Nu* makes a jump to its final value. As *Br* increases, the jump occurs at a shorter distance from the entrance. Since the wall temperature is constant, they all converge to the same fully developed value, although the Nusselt number is greater for larger values of the Brinkman number in the developing range. This effect can be explained by the driving mechanism for heat transfer, which is the difference between the temperatures of the bulk fluid and the wall. In the present case, *Br* is positive. In other words, fluid is being cooled. The fluid temperature becomes closer to the wall temperature as it flows through the channel. When we include viscous heating, fluid temperature takes higher values, which increases the temperature difference between the fluid and the wall and thus heat transfer.

Since the definition of the Brinkman number is different for the uniform heat flux boundary condition case, a positive *Br* means that the heat is transferred to the fluid from the wall as opposed to the uniform temperature case. Therefore, we see in Fig. 5 that *Nu* decreases as *Br* increases when $Br > 0$.

In Fig. 6, the variation of the fully developed *Nu* with *Kn* for these two cases, with and without viscous heating, is given. It is seen from the figure that, for the uniform temperature boundary condition at the wall *Kn* number increase due to the reduction of the channel size has more influence with the presence of viscous dissipation.

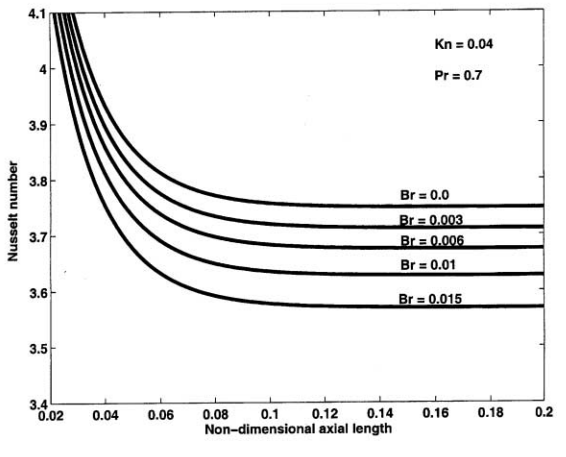

Fig. 5. The effect of viscous heating on heat transfer at the channel entrance for uniform heat flux at the wall.

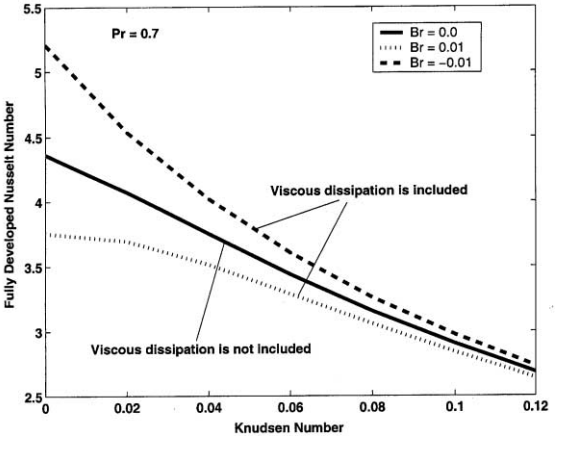

Fig. 7. Variation of the fully developed Nusselt number with Knudsen number with/without considering viscous heating for uniform heat flux at the wall.

Fig. 7 shows the effect of positive or negative Br values ($Br = \mp 0.01$) on heat transfer. As we mentioned before, for this type of boundary condition, a negative Br means that the fluid is being cooled. Therefore, the Nusselt number takes higher values for $Br < 0$ and lower values for $Br > 0$.

The fully developed Nusselt number values for all of the cases discussed here, are given in Tables 1–5.

Table 2
The fully developed Nusselt number values, $Br = 0.01$, constant T at the wall

$Br = 0.01$	$Pr = 0.6$	$Pr = 0.7$	$Pr = 0.8$	$Pr = 0.9$	$Pr = 1.0$
$Kn = 0.0$	6.4231	6.4231	6.4231	6.4231	6.4231
$Kn = 0.02$	5.3971	5.5639	5.6959	5.8031	5.8917
$Kn = 0.04$	4.5971	4.8446	5.0484	5.1291	5.3643
$Kn = 0.06$	3.9769	4.2592	4.4987	4.7044	4.8831
$Kn = 0.08$	3.4903	3.7838	4.0385	4.2615	4.4586
$Kn = 0.10$	3.1022	3.3947	3.6531	3.8830	4.0888
$Kn = 0.12$	2.7824	3.0729	3.2856	3.5589	3.7675

Table 3
The fully developed Nusselt number values, $Br = 0$, constant q at the wall

$Br = 0$	$Pr = 0.6$	$Pr = 0.7$	$Pr = 0.8$	$Pr = 0.9$	$Pr = 1.0$
$Kn = 0.0$	4.3627	4.3627	4.3627	4.3627	4.3627
$Kn = 0.02$	3.9801	4.0701	4.1403	4.1966	4.2428
$Kn = 0.04$	3.5984	3.7483	3.8692	3.9687	4.0521
$Kn = 0.06$	3.2519	3.4383	3.5927	3.7227	3.8337
$Kn = 0.08$	2.9487	3.1554	3.3306	3.4808	3.6112
$Kn = 0.10$	2.6868	2.9035	3.0904	3.2533	3.3966
$Kn = 0.12$	2.4613	2.6813	2.8739	3.0440	3.1953

Table 4
The fully developed Nusselt number values, $Br = 0.01$, constant q at the wall

$Br = 0.01$	$Pr = 0.6$	$Pr = 0.7$	$Pr = 0.8$	$Pr = 0.9$	$Pr = 1.0$
$Kn = 0.0$	4.0353	4.0353	4.0353	4.0353	4.0353
$Kn = 0.02$	3.7905	3.8720	3.9355	3.9863	4.0280
$Kn = 0.04$	3.4863	3.6268	3.7398	3.8327	3.9104
$Kn = 0.06$	3.1833	3.3617	3.5091	3.6331	3.7387
$Kn = 0.08$	2.9052	3.1056	3.2752	3.4204	3.5462
$Kn = 0.10$	2.6582	2.8701	3.0527	3.2115	3.3510
$Kn = 0.12$	2.4419	2.6583	2.8475	3.0144	3.1627

Table 5
The fully developed Nusselt number values, $Br = -0.01$, constant q at the wall

$Br = -0.01$	$Pr = 0.6$	$Pr = 0.7$	$Pr = 0.8$	$Pr = 0.9$	$Pr = 1.0$
$Kn = 0.0$	4.7481	4.7481	4.7481	4.7481	4.7481
$Kn = 0.02$	4.1898	4.2897	4.3677	4.4304	4.4819
$Kn = 0.04$	3.7181	3.8783	4.0078	4.1147	4.2044
$Kn = 0.06$	3.3236	3.9337	3.5185	3.6803	3.8169
$Kn = 0.08$	2.9935	3.2069	3.3879	3.5436	3.6787
$Kn = 0.10$	2.7160	2.9377	3.1292	3.2963	3.4434
$Kn = 0.12$	2.4810	2.7047	2.9008	3.0742	3.2286

References

[1] S.B. Choi, R.F. Barron, R.O. Warrington, Fluid flow and heat transfer in microtubes micromechanical sensors actuators and systems, ASME DSC 32 (1991) 123–134.

[2] J.C. Harley, Y. Huang, H.H. Bau, J.N. Zemel, Gas flow in micro-channels, J. Fluid Mech. 284 (1995) 257–274.

[3] A. Beskok, G.E. Karniadakis, Simulation of heat and momentum transfer in complex micro geometries, J. Theoret. Heat Transfer 8 (4) (1994) 647–653.

[4] E.B. Arkilic, K.S. Breuer, M.A. Schmidt, Gaseous flow in microchannels. In application of microfabrication to fluid mechanics, ASME FED 197 (1994) 57–66.

[5] J.C. Shih, C. Ho, J. Liu, Y. Tai, Monatomic and polyatomic gas flow through uniform microchannels, in: 1996 National Heat Transfer Conference, DSC 59, 1996, Micro Electro Mechanical Systems (MEMS), Atlanta, GA, USA, pp. 197–203.

[6] R.F. Barron, X. Wang, T.A. Ameel, R.O. Warrington, The Graetz problem extended to slip-flow, Int. J. Heat Mass Transfer 40 (8) (1997) 1817–1823.

[7] E.M. Sparrow, S.H. Lin, Laminar heat transfer in tubes under slip-flow conditions, J. Heat Transfer 84 (1962) 363–369.

[8] T.A. Ameel, R.F. Barron, X. Wang, R.O. Warrington, Laminar forced convection in a circular tube with constant heat flux and slip flow, Microscale Thermophys. Eng. 1 (4) (1997) 303–320.

[9] H.P. Kavehpour, M. Faghri, Y. Asako, Effects of compressibility and rarefaction on gaseous flows in microchannels, Numer. Heat Transfer Part A 32 (1997) 677–696.

[10] B. Vick, M.N. Ozisik, Y. Bayazitoglu, A method of analysis of low peclet number thermal entry region problems with axial conduction, Lett. Heat Mass Transfer 7 (1980) 235–248.

[11] Y. Bayazitoglu, N. Ozisik, On the solution of Graetz type problems with axial conduction, Int. J. Heat Mass Transfer 23 (1980) 1399–1402.